Botanical Sciences 99(2): 398-412 2021
DOI: 10.17129/botsci.2779

Received: October 23, 2020, Accepted: November 30, 2020
On line first: February 15, 2021

Structural Botany / Botánica Estructural

Phylogenetic placement of enigmatic *Astianthus* (Bignoniaceae) based on molecular data, wood and bark anatomy

Posición filogenética del enigmático género *Astianthus* (Bignoniaceae) con base en datos moleculares, de anatomía de madera y de corteza

Marcelo R. Pace[1]*, Brenda Hernández-Hernández[1], Esteban M. Martínez Salas[1], Lúcia G. Lohmann[2] and N. Ivalú Cacho[1]*

[1] Universidad Nacional Autónoma de México, Instituto de Biología, Departamento de Botánica, Ciudad Universitaria, Coyoacán, Mexico City, Mexico.
[2] Universidade de São Paulo, Instituto de Biociências, Departamento de Botânica, Cidade Universitária, São Paulo, SP, Brazil.
*Authors for correspondence: marcelo.pace@ib.unam.mx, ivalu.cacho@gmail.com

Abstract

Background: *Astianthus* is a monospecific arborescent genus of Bignoniaceae that occur in the Pacific Coast of central Mexico and northern Central America, where it grows in dense populations along riversides. Its phylogenetic placement has remained controversial since *Astianthus* has unusual morphological characters such as a four-loculed ovary, and simple, pulvinate, verticillate leaves.

Methods: Here we used three plastid markers *ndh*F, *rbc*L, and *trn*L-F, wood, and bark anatomical data to investigate the phylogenetic placement of *Astianthus* and assign it to one of Bignoniaceae's main clades.

Results: Our molecular phylogenetic analyses indicated that *Astianthus* belongs in tribe Tecomeae *s.s.*, where other charismatic Neotropical Bignoniaceae genera such as *Campsis* and *Tecoma* are currently placed. Wood and bark anatomy support this placement, as *Astianthus* reunites a unique combination of features only known from members of Tecomeae *s.s.*, such as storied axial parenchyma, the co-occurrence of homo- and heterocellular rays, septate fibers, and scattered phloem fibers in the bark.

Conclusions: The placement of *Astianthus* within Tecomeae *s.s.* provides further support to previous proposals for the Neotropical origin of this Pantropical tribe.

Keywords: Catalpeae, Lamiales, plant anatomy, secondary phloem, secondary xylem, Tecomeae.

Resumen

Antecedetes: *Astianthus* es un género monoespecífico y arborescente de Bignoniaceae cuya distribución abarca la porción occidental del centro de México y norte de Centroamérica. *Astianthus* suele crecer en poblaciones densas en ambientes riparios. La ubicación filogenética de *Astianthus* ha permanecido controversial, debido a que presenta una combinación de caracteres morfológicos que es inusual en la familia: ovario tetra-locular y hojas simples, verticiladas y pulvinadas.

Métodos: Se utilizó una combinación de tres marcadores del plástido (*ndh*F, *rbc*L y *trn*L-F) así como datos anatómicos de madera y corteza para investigar la posición filogenética de *Astianthus*, y determinar su asignación a uno de los clados principales de Bignonicaceae.

Resultados: Nuestros análisis filogenéticos indican que *Astianthus* pertenece a la tribu Tecomeae *s.s.*, en la cual se encuentran otros géneros neotropicales y carismáticos de Bignoniaceae, como *Campsis* y *Tecoma*. La anatomía de madera y corteza apoyan los resultados moleculares, pues *Astianthus* reúne una combinación única de características que sólo se conocen de otros miembros de Tecomeae *s.s.*, tales como parénquima axial estratificado, la co-ocurrencia de radios homo- y heteroceluares, fibras septadas y fibras individuales dispersas en el floema.

Conclusiones: La ubicación filogenética de *Astianthus* como parte de Tecomeae *s.s.* proporciona evidencia que apoya la hipótesis de un origen neotropical de esta tribu pantropical.

Palabras clave: Catalpeae, floema secundario, Lamiales, Tecomeae, xilema secundario.

In the past decades our knowledge of phylogenetic relationships within members of the Bignoniaceae has improved substantially thanks of phylogenetic reconstructions based on molecular data to the entire family (Spangler & Olmstead 1999, Olmstead *et al*. 2009), its main tribes (Zjhra *et al*. 2004, Lohmann 2006, Grose & Olmstead 2007a, Li 2008, Callmander *et al*. 2016, Ragsac *et al*. 2019), or key genera (Kaehler *et al*. 2012, 2019, Fonseca & Lohmann 2015, Medeiros & Lohmann 2015, Fonseca & Lohmann 2018, Thode *et al*. 2019, Carvalho-Francisco & Lohmann 2020). These phylogenetic reconstructions formed the basis for a series of new taxonomic treatments for the family (Grose & Olmstead 2007b, Lohmann & Taylor 2014). However, the phylogenetic placement of taxa that combine a narrow distribution and a rather ambiguous morphology has remained uncertain (Pace *et al*. 2016). *Astianthus* D.Don is one of such examples. This monotypic genus only includes *Astianthus viminalis* (Kunth) Baill. (Figure 1), a species distributed across the Pacific Coast side of central and southern Mexico and northern Central America (El Salvador, Guatemala, Honduras, and Nicaragua), typically associated to riparian habitats (Gentry 1980, 1992). Because of its amenable stature, attractive perennial foliage, and intense flowering, *A. viminalis* is sometimes planted as an ornamental along streets in southern Mexico. This species is also used in medicine, especially to treat diabetes (Meckes *et al*. 2001, Pérez-Gutiérrez *et al*. 2009).

Regardless of the economic importance detailed above, *Astianthus* taxonomic placement has remained controversial due to its unusual morphological features such as the verticillate pulvinate, simple leaves (Figure 1C) , and the 4-loculed ovary derived from the formation of a false septum in addition to the regular septum found in other Bignoniaceae (Gentry 1980, 1992). Within the Bignoniaceae, verticillate, simple leaves are found elsewhere in members of tribe Catalpeae, such as *Catalpa* Scop. and *Chilopsis* D. Don, and a few other scattered genera or individual species across the family. Two other genera that share these traits, *Deplanchea* Vieill. and *Delostoma* D.Don, were previously placed in the Tecomeae *s.l.,* While the former is currently included in Tecomeae *s.s.* (Olmstead *et al*. 2009), the latter remains unplaced as it has emerged with low support as its own single lineage and sister to the bulk of the Bignoniaceae (Olmstead *et al*. 2009). Four-loculed ovaries are also rare in the family, and are only known to occur in two other genera: *Tourrettia* DC., a herbaceous vine in the Andean tribe Tourrettieae, and *Heterophragma* DC., an Asian tree, previously included in the Tecomeae *s.l.* (Fischer *et al*. 2004), but currently placed within the Paleotropical clade (Olmstead *et al*. 2009).

In addition to the simple, pulvinate, entire, verticillate leaves (Figure 1C, E-F) and a 4-loculed ovary, *Astianthus viminalis* is also recognized for being a tree with rough bark (Figure 1A-B), 10 to 25 m high, generally occurring in dense populations (Gentry 1992) - the species is sometimes also described as a shrub (Fischer *et al*. 2004). Since *Astianthus* commonly grows near rivers and streams, flowering and fruiting branches sprouting from subterranean stoloniferous roots can result in a shrubby aspect (as observed by E.M.M.S.). *Astianthus* has terminal, paniculate inflorescences (Figure 1E), campanulate flowers, 5-dentate calyces (Figure 1D), and tubular-infundibuliform yellow corollas (Figure 1D). The capsular fruits are reddish-green, terete, fusiform, and glabrous (Figure 1F), with winged seeds borne perpendicularly on the septum and parallel to the false septum (Gentry 1992).

The genus *Astianthus* was initially placed by De Candolle (1838) in the Eubignonieae, a group that contained all Bignoniaceae with septicidal capsules (*i.e*., fruit dehiscence parallel to the septum). This placement was likely due to *Astianthus*' false additional septum and the genus was subsequently transferred to Catalpeae *sensu* De Candolle (1845). This tribe included the Bignoniaceae with loculicidal capsules (*i.e*., fruit dehiscence perpendicular to the septum), consistent with its real septum. Also based on the loculicidal capsules, Bentham & Hooker (1876) subsequently transferred *Astianthus* to Tecomeae, a classification continued by Gentry (1992).

As currently circumscribed, Tecomeae *s.s.* includes 12 genera distributed worldwide, in both the Northern and the Southern hemispheres, while other members of Tecomeae *s.l.* are now placed within Catalpeae, Jacarandeae, the Paleotropical clade (including the Malagasy tribe Coleae), and the Neotropical *Tabebuia* alliance (including tribe Crescentieae) (Olmstead *et al*. 2009). Based on the Neotropical distribution and morphology (*e.g.,* simple, verticillate leaves, and loculicidal capsule), *Astianthus* seems to fit best within Catalpeae, an exclusively North American tribe resurrected from De Candolle's Prodromus (1845). However, *Astianthus* has a false septum, a feature not found in any Catalpeae. The morphological similarity between *Astianthus* and members of Catalpeae, especially the sympatric *Chilopsis*, was noted previously (Gentry 1992). However, Gentry (1992) noted that *Astianthus* was even more similar to *Tecoma* Juss., with which it shares similar flowers, fruits, and geographical distribution. On the other hand,

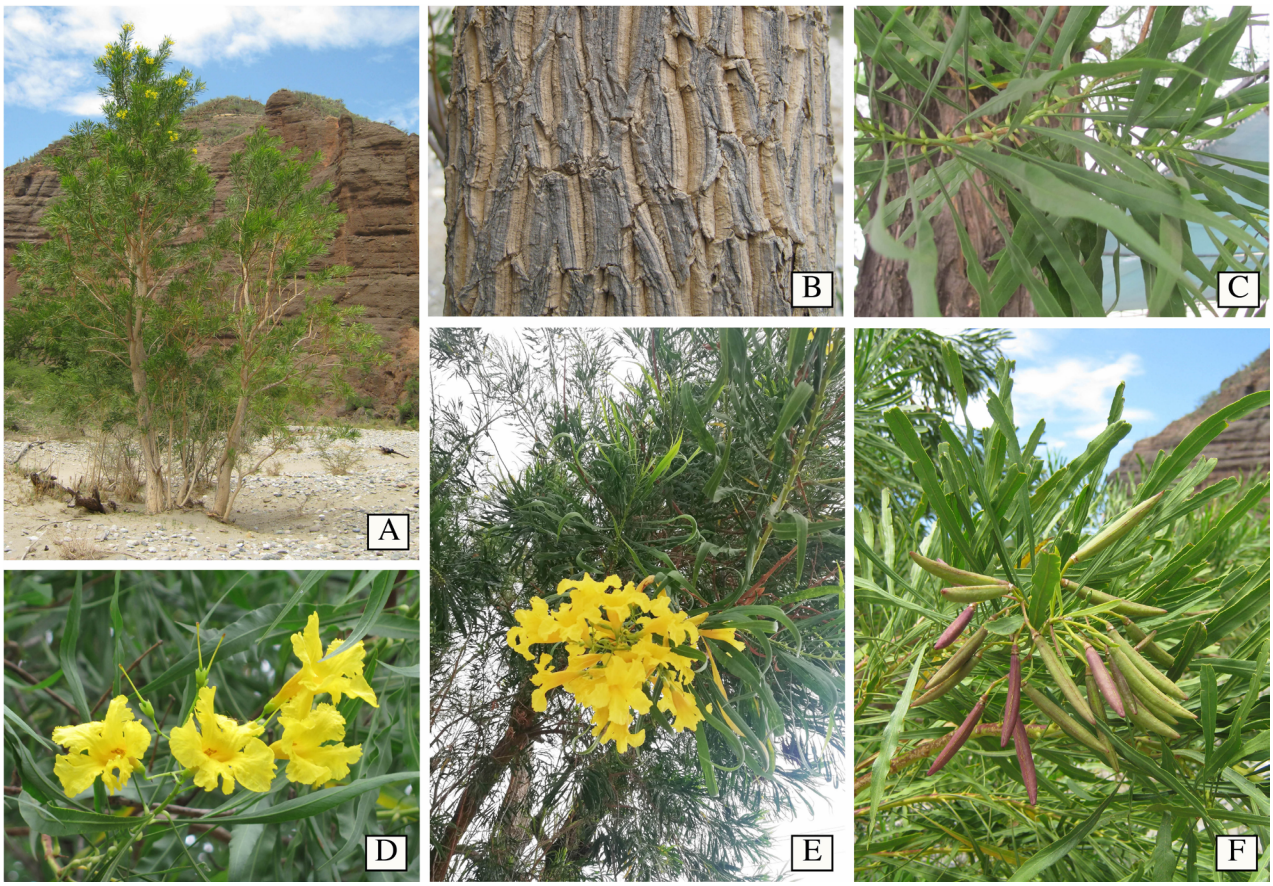

Figure 1. General morphology of *Astianthus*. A. Plant habit, a tree approximately 15 m high, growing in Cuicatlán, Oaxaca, Mexico. B. Rough bark. C. Simple, pulvinate, entire, verticillate leaves. D. Yellow, campanulate flowers, calyx with five acute triangular teeth, and tubular infundibuliform corolla. E. Terminal, paniculate inflorescence. F. Reddish terete capsules in a terminal infructescence. Image credits: A-B, F Esteban Martínez; C-D Carlos Cavazos; E, Carlos Domínguez-Rodríguez.

Tecoma is nowadays included in Tecomeae *s.s.* which predominantly includes lianas, shrubs, and treelets with pinnately compound leaves (Olmstead *et al.* 2009), although some species are trees with simple leaves (Gentry 1992).

In addition to molecular systematic studies, wood anatomy has been central in the understanding of taxonomic affinities within Bignoniaceae and delimiting synapomorphies to different lineages (Pace *et al.* 2009, 2015a, b, 2016). Even in pre-molecular times, the presence of variant secondary growth was recognized as unique to tribe Bignonieae (Crüger 1850, Schenck 1893), and this feature was used to circumscribe species in and out of this tribe (Gentry 1980, Lohmann 2006). Also, wood anatomical differences previously described for large genera of Bignoniaceae were later shown to match clade subdivisions found in molecular studies. The genus *Tabebuia s.l.* is a prime example. It was extensively studied by wood anatomists given its economically important timber (Record & Hess 1943), and three very distinctive groups were established based on their wood characters: (i) those very hard, durable *Tabebuia* Gomes ex DC. woods used in carpentry, (ii) those of light wood used in the transport of fruit and vegetables locally called as *caixeta*, and (iii) those with woods anatomically intermediate between the previous two groups (Record & Hess 1943, Dos Santos & Miller 1992). A molecular phylogenetic study provided additional support for these same three groups (Grose & Olmstead 2007a), leading to a new generic classification (Grose & Olmstead 2007b). Under the new system, the species with light wood were maintained in *Tabebuia*, while those with hard wood were transferred to *Handroanthus* Mattos, with some species of intermediate woods included in *Roseodendron* Miranda (Grose & Olmstead 2007a, b). Not all species of intermediate woods have yet been studied to date in order to verify their taxonomic placement. Other examples of wood anatomical traits being of phylogenetic value within the Bignoniaceae abound: the

Table 1. Specimens of *Astianthus viminalis* and relatives which were exclusively sampled for this study. Herbarium abbreviations follow Thiers (2017). All other species sampled and their complete collection information can be found in Olmstead *et al.* (2009).

Species	Collector and number	Locality in Mexico	Used in molecular analyses	Used in anatomical analysis	Herbaria
Astianthus viminalis	M.R. Pace 895	Oaxaca, Huatulco, La Crucecita, Lecho del Río	Yes	Yes	MEXU, SPF, MO, US
Astianthus viminalis	J. Barajas Morales 408	Jalisco, La Huerta, Estación Biológica de Chamela	No	Yes	MEXU
Astianthus viminalis	J. Barajas Morales 531	Puebla, Coxcatlán, Lecho del Río Calipan	No	Yes	MEXU
Astianthus viminalis	J. C. Soto N. 18603	Guerrero, Zirándaro, cauce del Río del Oro	Yes	No	MEXU
Astianthus viminalis	C. Rojas-Martínez 107	Puebla, Río Tizac, selva baja caducifolia	Yes	No	MEXU
Bignonia potosina	M.R. Pace 818	Tabasco, Balancán, Margen del Río Usumacinta	Yes	No	MEXU, SPF
Tecoma stans	M.R. Pace 906	Ciudad de México, Instituto de Biología, Ornamental	Yes	No	MEXU

differences in ray width and composition are useful in delimiting two main clades within tribe Jacarandeae. In this latter, it is remarkable that *Jacaranda copaia* (Aubl.) D.Don, the only species with anatomically intermediate wood, forms a separate lineage (Dos Santos & Miller 1997, Ragsac *et al.* 2019). There are also wood characters that consistently help delimit the clades most similar to *Astianthus*, *i.e.*, Catalpeae and Tecomeae *s.s*. The Catalpeae has unique simple to semi bordered pits and abundant tyloses, while Tecomeae *s.s.* has the unique combination of rays with body cells procumbent and marginal cells square to upright, a tendency to a storied structure, and scanty paratracheal to aliform parenchyma (Pace *et al.* 2015a).

Given the importance of both molecular phylogenetic data, wood and bark anatomical characters for Bignoniaceae systematics, we combine both types of evidence to unravel the enigmatic phylogenetic placement of *Astianthus*.

Material and methods

We collected samples of *Astianthus viminalis* for anatomical and phylogenetic studies in the field. To broaden our geographic sampling, we included additional samples of *A. viminalis* from the National Herbarium of Mexico and its wood collection (MEXU; see Table 1). To determine the phylogenetic placement of *Astianthus*, we generated sequences of *A. viminalis*, as well as sequences of *Bignonia potosina* (K. Schum. & Loes.) L.G. Lohmann, and *Tecoma stans* (L.) Juss. ex Kunth for this study (see Table 1 for collection or specimen information). All other sequences of ingroup and outgroup taxa were the same as those used in Olmstead *et al.* (2009; a complete list with voucher information and GenBank accession numbers can be found in this study). We also included 25 additional sequences from taxa available on GenBank (Supplementary material 1, Tabla S1) to fill gaps in *rbc*L sequences from the original sampling.

DNA extraction, amplification, and sequencing. We extracted DNA using the DNeasy Plant Mini Kit (Qiagen, Valencia, California) from either silica-dried plant material, fresh material, or herbarium specimens, following the manufacturer's protocols.

For each accession, we amplified portions of the *ndh*F and *rbc*L genes and the *trn*L-F spacer. These three regions from the plastid genome have been useful to estimate phylogenetic relationships within the Bignoniaceae at the tribal (Olmstead *et al.* 2009), generic (Lohmann 2006), and species (*e.g.,* Fonseca & Lohmann 2015, Carvalho-Francisco & Lohmann 2020) levels. We sequenced the *ndh*F marker in two pieces, using the PCR primer pairs 5F-1318R and 972F-3R described in an earlier study (Olmstead & Sweere 1994). For the *trn*L-F region, we used primers C and F (Taberlet *et al.* 1991), and for *rbc*L, we used F and R primers previously described (Hipkins *et al.* 1990, Supplementary material 2, Figure S1). PCR reactions were prepared by adding each primer at 1mM to Go-

Taq® Green Master Mix (Promega M1722), and adjusting with ddH_20 for a final volume of 25µL. PCR conditions consisted of an initial denaturation of 90s at 96 ºC, followed by 35 cycles of 30s at 95 ºC, 60s at 55 ºC, 60s at 72 ºC, and a final extension of 4min at 72 ºC. Upon completion, PRC products were run in a 1% agarose gel and assessed for size and quality in a UV transilluminator using gel red (Biotium 41003, Hayward, California).

Sanger sequencing was carried out at the National Biodiversity Laboratory (LaNaBio) at the Institute of Biology, UNAM, Mexico, in both directions. Briefly, sequencing reactions were prepared using BigDye Terminator 3.1 (Applied Biosystems), and run for 30 cycles consisting of 10s at 96 °C, 5s at 50 ºC, and 4 min at 60 ºC. Samples were cleaned using Centri-Sep plates (Thermo Fisher Scientific, Waltham, Massachusetts) following the manufacturer's directions. Samples were analyzed in an Applied Biosystems ABI 3730xl 96-capillary DNA analyzer (ThermoFisher Scientific, Waltham, Massachusetts).

Sequence editing and alignment. We examined and edited raw chromatograms for all newly generated sequences in Sequencher 5.4.6 (Gene Codes, Ann Arbor, Michigan). Contigs were assembled using default settings without lowering the threshold. We aligned each region individually and manually in Mesquite 3.5 (Maddison & Maddison

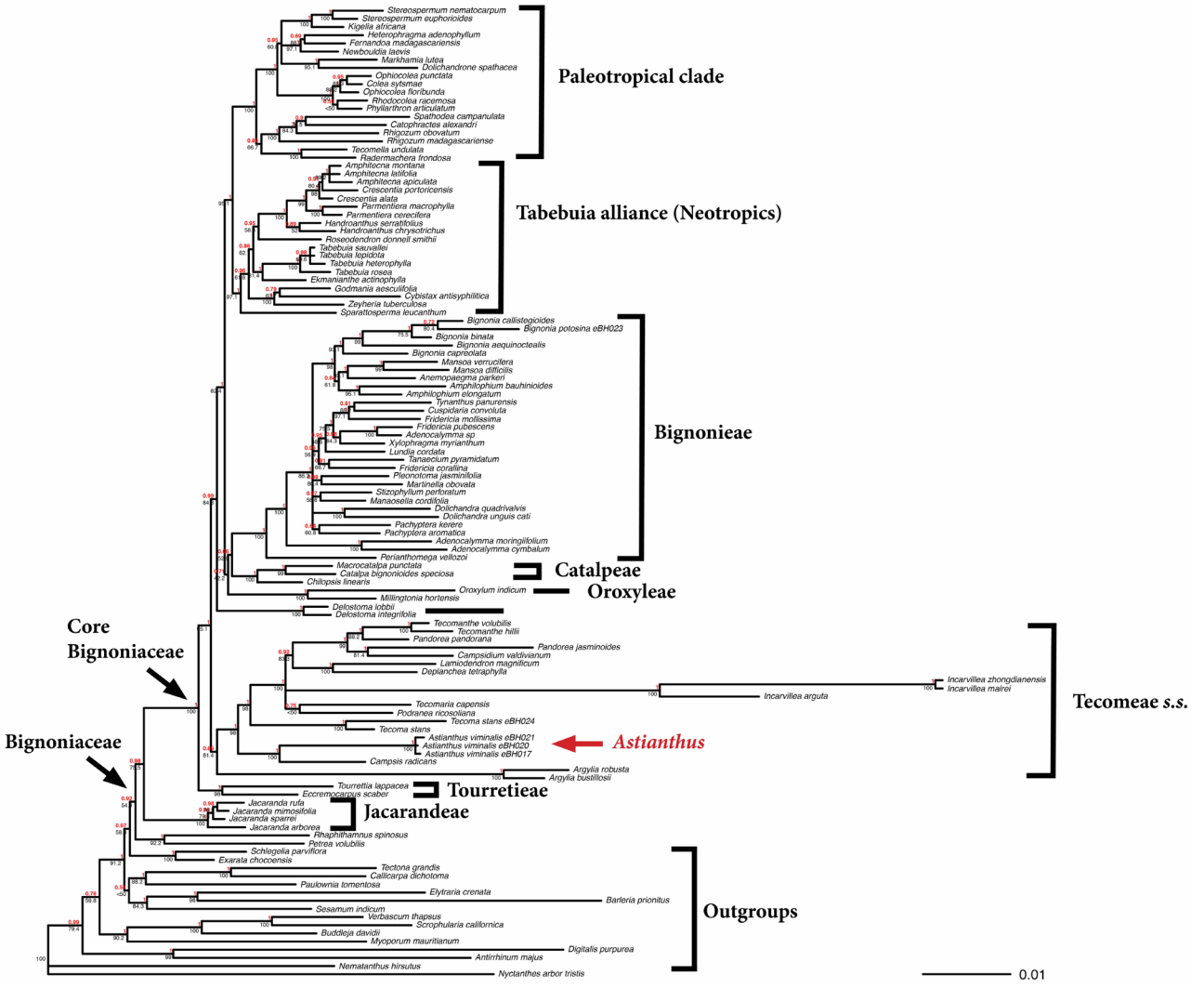

Figure 2. Consensus tree derived from a 20 million generation Bayesian analysis of the concatenated dataset (*ndh*F, *rbc*L, *trn*L-F). Both Bayesian Inference and Maximum Likelihood analyses strongly support *Astianthus* as sister to *Campsis*, within the Tecomae *s.s*. Posterior probabilities are provided in bold above branches and maximum likelihood bootstrap values in regular font below branches.

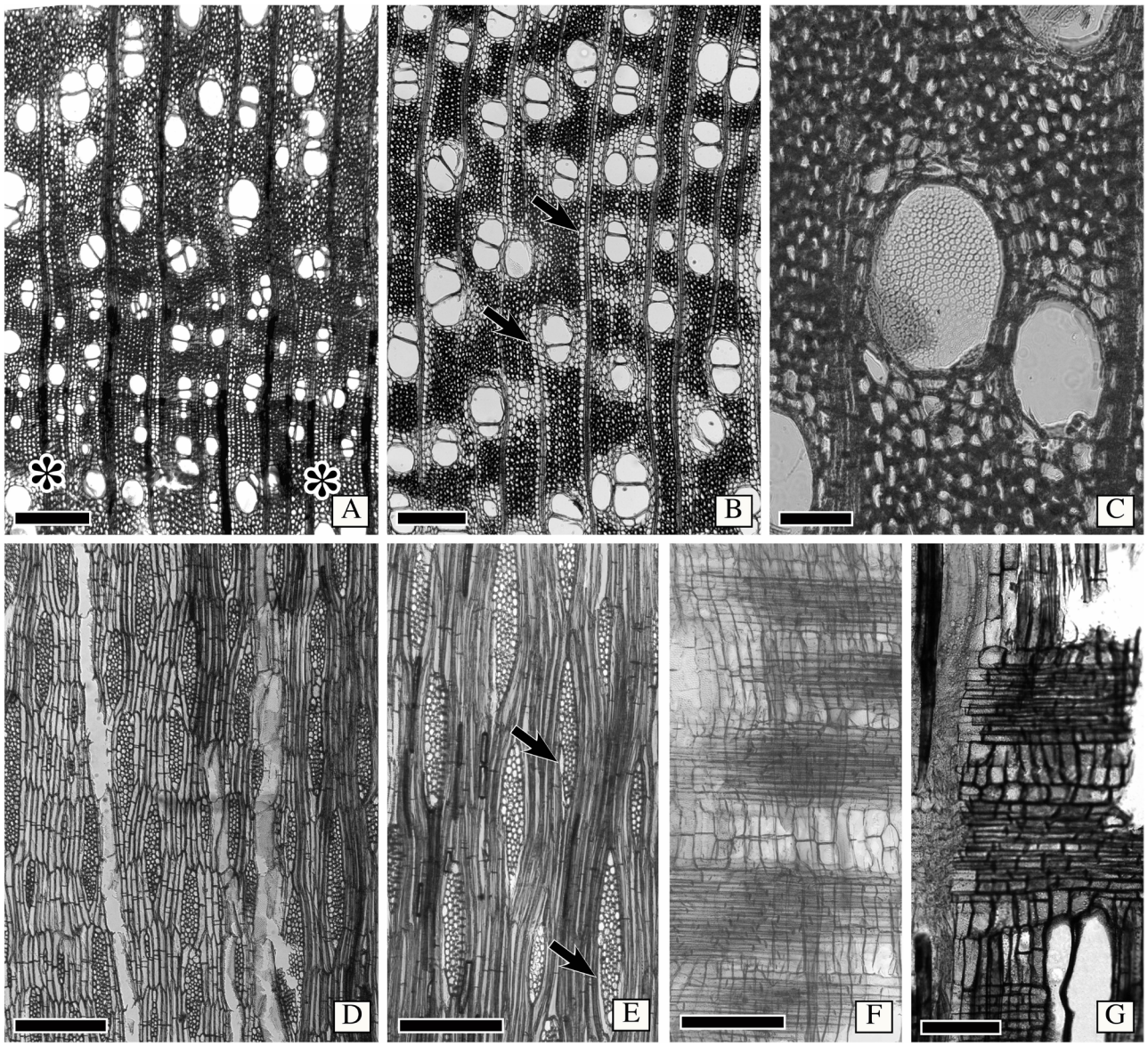

Figure 3. Wood anatomy of *Astianthus*. A-B. Transverse section. Semi-ring porous wood, growth rings delimited by narrower vessels, and radially narrow fibers (asterisks). Vessels solitary to multiples of 2-3. Clusters sometimes present. Fibers thin to thick walled. Axial parenchyma aliform with short confluences, some confluences also marginating the rays (arrows). C. Foraminate perforation plate in wide vessel, as seen in transverse section. D. Longitudinal tangential section. Parenchyma cells storied, with 2-(3-)cells per parenchyma strand. Rays 3-4 cells in width. E. Longitudinal tangential section. Note sheath cells present (arrows) and the septate fibers. F. Longitudinal radial section. Homocellular rays, with procumbent cells only. G. Heterocellular rays, with body composed of procumbent cells and a row of marginal square to upright cells. Scale bars: A-B, D = 400 µm, C = 100 µm, E-F = 300 µm, G = 150 µm.

2011), giving preference to transitions over transversions. All sequences generated for this study are available in GenBank with the following accession numbers: MT235272-MT235276 (*rbc*L), MT232737-MT232741(*ndh*F), and MW291155-MW291159 (*trn*L-F).

Phylogenetic analyses. We assessed evolutionary models for each region separately using jModelTest 2.1.7 (Darriba *et al.* 2012), and the Akaike information criterion (AIC; Akaike 1974). We analyzed each dataset separately and in combination, following a total evidence approach (Kluge 1989).

We conducted Maximum Likelihood analyses using RAxML-HPC (Stamatakis 2014) as implemented in the XSEDE tool in CIPRES (Miller *et al.* 2010), using a random seed (-p) of 12345, and the default (25) number of distinct rate categories (-c). For each analysis, matrices

Table 2. Diagnostics of data matrices used for phylogenetic analyses. PIC = Parsimoniously Informative Character.

Dataset	n taxa	n characters	constant characters	variable, no PIC	PIC	frequency no PICs	frequency PICs
*ndh*F	117	2,176	1,053	445	678	0.205	0.312
*rbc*L	69	1,426	1,057	176	193	0.123	0.135
*trn*L-F	112	1,233	666	278	289	0.225	0.234
concatenated	119	4,835	2,776	899	1,160	0.186	0.240

were run according to the model selected and the slow ML search algorithm. For the combined analyses including data from all three partitions (*ndh*F, *rbc*L, and *trn*L-F), we allowed for a mixed model (also slow search algorithm). Bootstrap analyses (100 replicates) were performed with the RAXML fast bootstrap algorithm implemented in CIPRES.

Bayesian analyses were run in MrBayes 3.2 (Ronquist *et al.* 2012), as implemented in CIPRES. An initial 5 million generation analysis was run using the selected model for each region to optimize parameters (including temperature) and ensure that the chains were running properly and reached stationarity. We checked chain swap information and parameter acceptance rates to ensure that parameters were acceptable (between 0.1 and 0.7), making sure all parameters had an ESS > 200, and examined appropriate chain behavior in Tracer 1.7.1 (Rambaut *et al.* 2018). We then conducted a second run including 20 million generations for each of our analyses. For the analyses with the concatenated dataset, the parameters associated with the model of evolution (Revmat, Statefreq, and Shape) were unlinked, while the ratemultipler, the topology and the branch lengths were linked across partitions. For all analyses, we implemented a temperature of 0.1 for the cold chain to ensure appropriate mixing. We sampled every 1,000 generations, and eliminated 25 % of the trees as burn-in. Sampling of the parameter space by the MCMC chains was summarized using the .sump and .sumt commands, while trees were visualized in FigTree 1.4.3 (Rambaut 2010).

We conducted all analyses on the Cyberinfrastructure for Phylogenetic Research cluster (CIPRES; Miller *et al.* 2010), which is housed at the San Diego Supercomputer Center (www.phylo.org/), and tree visualization and annotation was performed in R (R Core Team 2020).

Anatomical sampling and methods. Woods pulled from the MEXU xylarium were rehydrated in boiling water and glycerin for two hours following Pace (2019). All samples were softened in 4 % ethylenediamine for two days within a paraffin oven (Carlquist 1982). Anatomical sections of the transverse, longitudinal radial and longitudinal tangential planes were performed with the aid of a sliding microtome and permanent steel knives sharpened with sandpapers of different grids (Barbosa *et al.* 2018). Wood sections were obtained from unembedded materials and stained in 1 % aqueous safranin. Samples with cambium and bark underwent a previous step, being gradually embedded in polyethylene glycol 1500 (Rupp 1964), and subsequently sectioned with the aid of an anti-tearing coat of a polystyrene resin (Barbosa *et al.* 2010). The latter were double-stained for 15 minutes in Safrablau (Bukatsch 1972, modified by Kraus & Arduin 1997). All sections were dehydrated in an ethanolic series, with butyl acetate being used in the last step, and mounted in Canada Balsam to make permanent slides.

Wood descriptions followed the IAWA Committee for hardwood (IAWA Committee 1989), IAWA Committee for bark features (Angyalossy *et al.* 2016), and Carlquist (2001), adjusting to the specificities of the family whenever needed. Measurements were performed using ImageJ 1.52a (National Institute of Health, USA, www.imagej.nih.gov/ij, Rasband 2012). Since approximately half of the Bignoniaceae family is composed of lianas, and it has been well-documented that lianas tend to converge to similar anatomies (Carlquist 1985, Angyalossy *et al.* 2012, 2015, Chery *et al.* 2020), we focused the comparison of *Astianthus* with shrub and tree members of the family.

Results

Phylogenetic placement of Astianthus. A summary of our individual and combined data matrices, including dimension, number of variable and parsimony informative characters are presented in Table 2. The GTR + gamma was

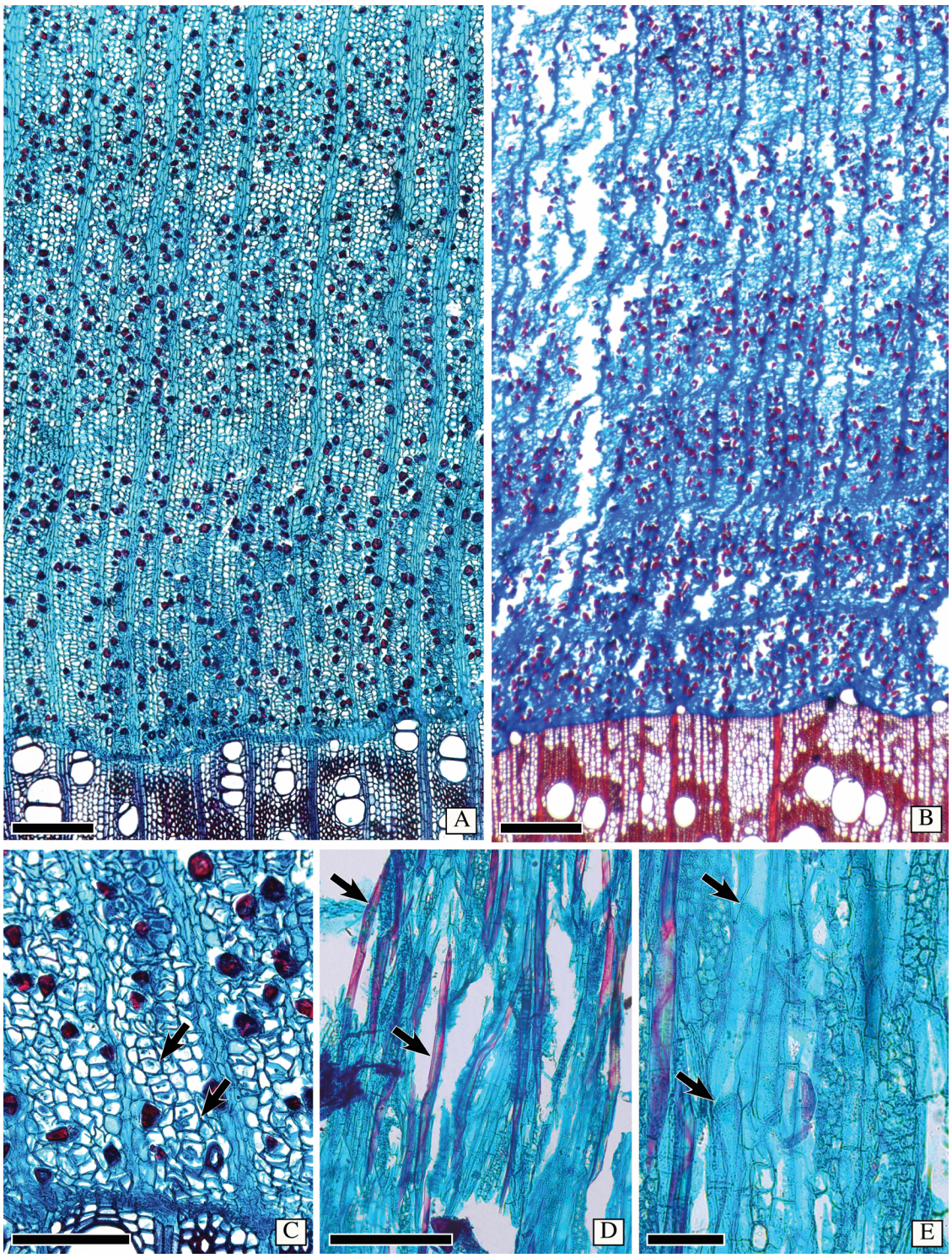

Figure 4. Secondary phloem of *Astianthus* and *Campsis*. A, C-E. *Astianthus*. B. *Campsis*. A. Secondary phloem non-stratified, diffuse fibers scattered across the entire tissue. Course of rays straight. Transverse section (TS). B. Secondary phloem non-stratified, with diffuse fibers scattered across the entire tissue. Ray course slightly undulated. TS. C. Sieve tubes in radial multiples of 2-4 common, diffuse fibers, differentiating close to the cambial region. Either one companion cell laying on one side of the sieve tube (lower arrow), or two companion cells, lying on opposite sides of the sieve tube (upper arrow). TS. D-E. Longitudinal tangential section. Fibers isolated, tapering (arrows). E. Sieve tube elements with simple, slightly inclined sieve plates (arrows). Scale bars: A-B = 300 µm, C-D = 200 µm, E = 100 µm.

recovered as the best model of DNA substitution in all analyses and implemented for all datasets.

The results of the Bayesian and Maximum Likelihood analyses of the combined datasets are largely congruent with those of Olmstead *et al.* (2009) and Lohmann (2006), including strong support for the tribes within Bignoniaceae as well as the family (Figure 2).

Our phylogenetic combined analyses based on Maximum Likelihood (ln = -38901.785924) and Bayesian Inference frameworks led almost identical topologies with minor differences not related to the placement of *Astianthus*, therefore only the consensus Bayesian tree is shown (Figure 2; the ML tree is available in Supplementary material 2, Figure S1). In all analyses, *Astianthus* is strongly supported as monophyletic (1.0 PP, 100 % ML BS). *Astianthus* falls within the Core Bignoniaceae clade (1.0 PP, 100 % ML BS; *sensu* Olmstead *et al.* 2009), within tribe Tecomeae *s.s.* (1.0 PP, 98 % ML BS), and sister to *Campsis radicans* (L.) Bureau (1.0 PP, 100 % ML BS).

Wood anatomy of Astianthus. Growth rings distinct, delimited by narrower vessels and radially narrow fibers (Figure 3A). Wood semi-ring porous (Figure 3A). Vessels without a specific arrangement, solitary or in radial multiples of 2-3 (Figure 3A-B), clusters of 3-4 vessels common, perforation plates simple, some wide vessel elements with foraminate perforation plate on horizontal end walls (Figure 3C). Intervessel pits alternate, minute (6 µm), vessel-ray pitting with distinct borders, similar to intervessel pits in size and shape throughout the ray cell, helical thickening absent. Vessel diameter 117 ± 32 µm, frequency 14 ± 3 vessels/mm^2, two vessels per group, vessel length 258 ± 38 µm. Tyloses and deposits absent both in sapwood and hardwood. Fibers thin to thick walled (Figure 3A-C, E), with simple to minute bordered pits, septate fibers present (Figure 3E). Axial parenchyma vasicentric to aliform with short confluences (Figure 3A-B), and confluences marginating the rays (Figure 3B), with 2-4 cells per parenchyma strand (Figure 3D). Rays 3-4-seriate (Figure 3D-E), longitudinal merging of two rays common, rays lower than 1 mm. Rays either homocellular with procumbent cells only (Figure 3F) or heterocellular, with body composed of procumbent cells and one row of square marginal cells (Figure 3G). Sheath cells common (Figure 3E). Axial parenchyma cells storied (Figure 3D), and in certain areas narrow vessels also storied, but not conspicuously (storied fusiform cambial initials). Crystals absent.

Bark anatomy of Astianthus. *Secondary phloem*. Non-stratified phloem (Figure 4A). Conducting phloem with sieve tubes solitary or in radial multiples of 2-4 (Figure 4 C). All sieve plates simple, on a transverse wall (Figure 4E). Sieve tube area 436 ± 136 µm^2, diameter 24 ± 13 µm, and sieve element length of 259 ± 24 µm. One companion cell lying on the corner of the sieve tube (Figure 4C) or sometimes with two companion cells lying on opposite sides of the sieve tube (Figure 4C), companion cells in strands of more than two cells. Parenchyma constituting the ground tissue (Figure 4A, C), parenchyma strands with 2-4 cells. Course of rays straight (Figure 4A). Ray width, height and composition equal to that of the wood (Figure 4E). Ray dilatation seemingly absent (Figure 4A). Sclerenchyma composed of fibers only, diffuse, either solitary or in multiples of two (Figure 4A, C-D), with a polygonal shape (Figure 4C), differentiating close to the cambium (Figure 4C). Axial parenchyma and sieve tube elements storied. Non-conducting phloem marked by sieve tubes and companion cells empty, collapsed. Dilatation phenomena practically restricted to cell enlargement, with not much cell division in both axial and ray parenchyma. No further sclerification.

Periderm. Rhytidome present, with many reticulate periderms. New periderms forming inside the secondary phloem, and enclosing large amounts of nonconducting phloem. Phellem cells evenly thin walled, non-stratified. Phelloderm cells are parenchymatous and thin walled (1-3 cell layer). No mineral inclusions recorded.

Discussion

Phylogenetic placement of Astianthus. The phylogeny of the Bignoniaceae reconstructed here indicates that *Astianthus* falls within Tecomeae *s.s.* With originally 12 genera, ca. 70 species and Pantropical distribution, Tecomeae *s.s.* is one of the most diverse tribes of the Bignoniaceae both in terms of morphology and distribution, with members ranging from latitudes 40° N to 40° S (Olmstead 2013) in Africa, Asia, the New World, and Oceania (Figure 5). Our analyses support *Astianthus* as sister to *Campsis* Lour., a lianescent genus with two species, one in eastern North America and one in China (Fischer *et al.* 2004). As currently circumscribed, tribe Tecomeae *s.s.* includes three main clades (Figure 5): the first clade includes the Andean herb *Argylia* D.Don, which is sister to the rest of the Tecomeae *s.s*; the second clade includes predominantly Neotropical species, with *Astianthus* and *Campsis* (except for the Chinese *Campsis grandiflora* (Thunb.) Schumann); the third clade consists of the rest of Tecome-

Table 3. Synopsis of the qualitative and quantitative wood features of Astianthus and all other lineages (tribes or major clades) in Bignoniaceae.

Tribe or clade		*ASTIANTHUS*	JACARANDEAE	TECOMEAE	*DELOSTOMA*	OROXYLEAE	CATALPEAE	BIGNONIEAE	TABEBUIA ALLIANCE	PALEOTROPICAL CLADE
Habit		Trees (sometimes shrubs)	Trees, and a few subshrubs in arid zones	Mostly lianas, with few trees and shrubs	Trees	Trees, a few lianas	Trees	Liana, a few shrubs	Trees	Trees and shrubs
Porosity		Semi – ring porous	Diffuse	Diffuse to ring – porous	Diffuse	Diffuse	Semi – ring porous	Diffuse to semi – ring porous	Diffuse	Diffuse
GROWTH RING MARKERS	**Marginal parenchyma**	–	+	±	+	+	+	+	+	+
	Radially flattened fibers	+	+	+	–	+	+	+	–	±
VESSELS	**Arrangement**	Diffuse	Diffuse	Diffuse	Radial pattern	Diffuse	Diffuse	Diffuse	Diffuse	Diffuse
	Grouping	Solitary to multiples of 2 – 3	Solitary to multiples of 2 – 3	Solitary to multiples of 2 – 3	Solitary to multiples of 2 – 3 & Radial multiples	Solitary to multiples of 2 – 3	Solitary to multiples of 2 – 3	Solitary to multiples of 2 – 3	Solitary to multiples of 2 – 3	Solitary to multiples of 2 – 3
	Vessel/group	2	1.23 – 2.11	1.93 – 5.32	2.93	1.24 – 1.94	1.33 – 1.56	1.31 – 4.73	1.24 – 2.22	1.08 – 2.58
	Dimorphism	–	–	+ in lianas	–	–	–	+	–	–
	Frequency (per mm²)	14 ± 3	10 – 21	6 – 320	46 ± 20	4 – 27	6 – 34	14 – 236	12 – 51	9 – 73
	Diameter (µm)	117 ± 32	68 – 75 (except for J. copaia with 300)	30 – 158	70 ± 12	80 – 179	131 – 204	45 – 293	44 – 125	51 – 178
	Tyloses	–	–	–	–	–	+	–	–	–
	Perforation plate	Simple and foraminate	Simple	Mostly Simple, some foraminate	Simple	Reticulate, foraminate and simple	Simple	Simple	Mostly Simple, some foraminate	Mostly Simple, some foraminate
	Helical thickening	–	–	+ in species ring – porous	–	–	+ in species semi – ring porous	–	–	–
	Intervessel pit size (µm)	6	7.2 – 10.3	4.3 – 9.4	3.1	3.1 – 5.3	4.1 – 11.1	2.6 – 12.4	2.5 – 19.1	2.2 – 10.7
AXIAL PARENCHYMA	**Patratracheal parenchyma**	Vasicentric to aliform	Aliform	Scanty to vasicentric	Scanty	Vasicentric to aliform	Scanty to aliform	Scanty to aliform	Aliform	Aliform
	Confluence	Short	Short to long	Absent from present	Absent	Short	Absent to short	Absent to short	Generally long, forming bands	Short to long
	Diffuse parenchyma	–	–	–	–	–	–	–	–	+ in Coleeae
	Parenchyma strands	Two – four	Four (3 – 4) cells per strand	Mostly four (3 – 4) cells per strand	Four (3 – 4) cells per strand	Four (3 – 4) cells per strand	Four (3 – 4) cells per strand	Four (3 – 4) cells per strand	2 – 4 cells per strand	Four (3 – 4) cells per strand
RAYS	**Ray height**	Short <1 mm	Short <1 mm	Short <1 mm and hight > 1mm in lianas	Short <1 mm	Short <1 mm	Short <1 mm	Generally high >1 mm, smaller in shrubs	Short <1 mm	Short <1 mm
	Ray width (in number of cells)	4 – Mar	1/2 – 3	2 – 3	3	3	3	1 – 9	1 – 3	1 – 3
	Rays: cellular composition	Mostly homocellular, some heterocellular	Homocellular in *Jacaranda* Monolobos and heterocellular in *Jacaranda* Dilobos	Heterocellular	Homo and hetero with 1 row of square cells	Homocellular	Homo and hetero with 1 row of square cells	Heterocellular mixed	Homocellular	Homo and hetero with 1 row of square cells
	Vessel – ray pitting	Similar to intervessel pits	Similar to intervessel pits	Similar to intervessel pits	Similar to intervessel pits	Similar to intervessel pits	Simple to semi – bordered	Predominantly similar to intervessel pits	Similar to intervessel pits	Similar to intervessel pits
	Perforated ray cells	–	–	+ in lianas	–	–	–	+	–	–
Septate fibers		+	–	+	+	±	±	+	–	–
Storied structure		+	–	–	–	–	–	– , present in but a few species	+	–
Crystals		–	Present in the rays of some species	Present in the rays of some species	Present in rays	–	Present in the rays of some species	Present in the rays of some species	When present, in both rays and axial parenchyma	Present in the rays of some species

ae *s.s.*, with members across the Neotropics, Africa, and Asia-Pacific (Fischer *et al.* 2004, Olmstead *et al.* 2009).

The placement of *Astianthus* within the same tribe as *Tecoma* corroborates Gentry's (1992) initial proposal that the leaf similarities between *Astianthus* and the Catalpeae genus *Chilopsis* represented a convergence to their riparian habit rather than an evidence of relatedness. On the other hand, the floral and fruit similarities shared between *Astianthus* and *Tecoma* were shown to corroborate phylogenetic findinds and earlier hypotheses of Gentry (1992). Both genera share many species with yellow flowers, a cupular, 5-dentate calyx, and linear capsular fruits (Fischer *et al.* 2004). *Tecoma* is composed of 14 species of shrubs to small trees distributed in tropical America from the Andes to Arizona (Gentry 1992, Fischer *et al.* 2004). Most *Tecoma* have pinnately compound leaves, but the genus contains also some species with simple leaves, such as *Tecoma castaneifolia* (D. Don) Melch. from Ecuador, *Tecoma tanaeciiflora* (Kranzlin) Sandwith from Bolivia and Peru, and some specimens of *T. weberbaueriana* from Peru and Ecuador. Furthermore, nearly all species with pinnately compound leaves of *Tecoma* usually have simple leaves at the base of all branches (Gentry 1992).

Wood and bark anatomy of Astianthus *in relation to other Bignoniaceae. Astianthus* shares many wood anatomical features with other tree members of the Bignoniaceae, such as the paratracheal parenchyma with a tendency to confluences, radially thick-walled fibers delimiting growth rings, short rays, a straight grain, and rare crystals (Table 3, Figure 5; Pace & Angyalossy 2013, Pace *et al.* 2015a, Gerolamo & Angyalossy 2017). The presence of foraminate perforation plates in wide vessels is not found in all Bignoniaceae but is scattered in at least eight different distantly related lineages across the entire family. This feature seems to be related to species growing under strongly seasonal rain regimes (Pace & Angyalossy 2013), a hypothesis that remains to be tested.

Considering less common anatomical attributes, *Astianthus* would still be a good fit in at least three different Bignoniaceae major clades: the Paleotropical clade, the *Tabebuia* alliance, and Tecomeae *s.s.* (Table 3). However, based on the Neotropical distribution, *Astianthus* is best placed in the *Tabebuia* alliance or Tecomeae *s.s.*. Members of both tribes can have a storied structure (although this feature is more common in the *Tabebuia* alliance) and homo to heterocellular rays (Pace *et al.* 2015a). However, the combination of these two features in addition to the

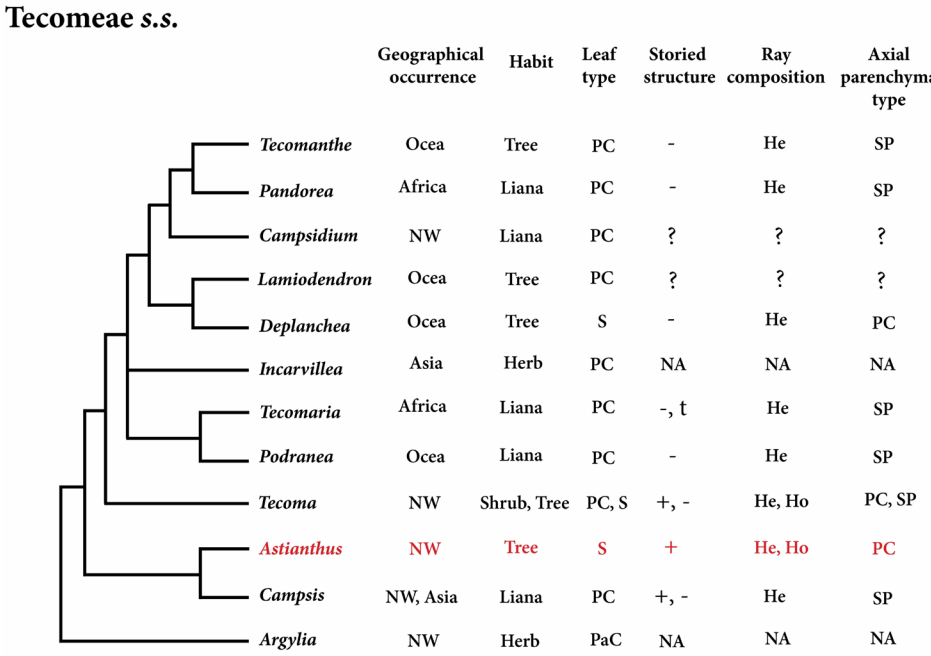

Figure 5. Phylogeny of Tecomeae s.s. with *Astianthus* highlighted in red. Feature comparisons. Geographical Occurrence (Africa, Asia, NW=New World, and Ocea = Oceania); Plant Habit (herb, liana, shrub or tree); Leaf Type (S = simple, PC = pinnately compound, PaC = palmately compound); Storied Structure (present or absent); Ray Composition (heterocellular and/or homocellular); Axial Parenchyma Type (PC = paratracheal confluent, SP = scanty paratracheal). NA = Not Applicable, plant without secondary growth. ? = unknown.

presence of septate fibers is found exclusively in Tecomeae *s.s.* (Table 3), supporting the phylogenetic placement suggested by the molecular data. The most notable differences between *Astianthus* and some members of Tecomeae *s.s.* (Figure 5) are likely associated to the difference of habits. Many of the genera of Tecomeae *s.s.* include lianas that seem to converge in a reduction in the wood axial parenchyma (Pace & Angyalossy 2013), contrary to what is found in lianas from other plant families (Angyalossy *et al.* 2015). In addition, in lianas in general the rays tend to become more heterocellular, similarly to what was seen in other Bignoniaceae, especially in the lianescent tribe Bignonieae (Pace & Angyalossy 2013).

The morphological similarity between *Astianthus* and members of the North American tribe Catalpeae is not mirrored by the wood anatomy. Members of Catalpeae are marked by a heartwood with abundant tyloses, a non-storied structure, and vessel to ray pits simple to slightly bordered (Pace *et al.* 2015a). On the other hand, *Astianthus* lacks tyloses, has storied axial parenchyma, and distinctly bordered vessel to ray pits.

The bark anatomy provides further support for the inclusion of *Astianthus* in Tecomeae *s.s.* Virtually all Bignoniaceae species studied thus far show a stratified bark, with clear fiber bands alternating with axial parenchyma and sieve tubes, regardless of the habit, ecological factors, or distribution (Roth 1981, Pace *et al.* 2011, 2015b). The single exception to this rule is *Campsis*, which emerged as sister to *Astianthus*, with whom it shares scattered single fibers across the entire phloem (Evert 2006, Figure 4B), a potential synapomorphy of this clade. This finding corroborates previous assumptions that the bark anatomy carries a strong phylogenetic signal in the family, independently of the habit, aiding the delimitation of major clades within the family (Pace *et al.* 2015b). Other bark features of *Astianthus* such as the presence of sieve tubes in radial multiples, axial parenchyma as a background tissue, a seemingly absent ray dilatation by cell divisions, and a reticulate rhytidome are more widespread in the family (Roth 1981, Pace *et al.* 2015b).

In conclusion, our phylogeny reconstruction based on three plastid markers (*ndh*F, *rbc*L, and *trn*L-F) indicates that *Astianthus* is nested within Tecomeae *s.s.*. This placement is further supported by the non-stratified bark, scattered bark fibers, storied axial parenchyma, homo and heterocellular rays co-occurring, and septate wood fibers. These results show the importance of combining in-depth studies of morphology and anatomy with molecular phylogenetic data for an improved understanding on plant diversification, especially in the tropics. The placement of *Astianthus* within Tecomeae *s.s.* further supports a neotropical origin for the tribe.

Acknowledgments

We thank the Laboratorio de Genómica Funcional y Sistemas (CONACyT INFR2016-268109), for access to equipment and infrastructure; Rosalinda Tapia López for reagents and advice; Laura Márquez and Nelly López from LaNaBio (Laboratorio Nacional de Biodiversidad) for sequencing services; Carlos Cavazos and Carlos Domínguez-Rodríguez for permission to use their pictures. Ivonne Garzón and Rosario Redonda for assistance in the field. Teresa Terrazas, and three anonymous reviewers and the editors for their careful revisions and suggestions that improved the manuscript. The curator of MEXU, Gerardo Salazar, for allowing removal of leaf and wood fragments from both the herbarium and wood collection. This work was supported by UNAM-PAPIIT IA200319 and IA200521. L.G.L. is supported by a CNPq pq-1B grant (310871/2017-4).

Supplementary material

Supplemental data for this article can be accessed here: https://doi.org/10.17129/botsci.2779

Literature cited

Akaike H. 1974. A new look at the statistical model identification. *IEEE Transactions on Automatic Control* **19**: 716-723. DOI: https://doi.org/10.1109/TAC.1974.1100705

Angyalossy V, Angeles G, Pace MR, Lima AC, Dias-Leme CL, Lohmann LG, Madero-Vega C. 2012. An overview of the anatomy, development, and evolution of the vascular system of lianas. *Plant Ecology and Diversity* **5**: 167-182. DOI: https://doi.org/10.1080/17550874.2011.615574

Angyalossy V, Pace MR, Lima AC. 2015. Liana anatomy: A broad perspective on structural evolution of the vascular system. *In*: Schnitzer SA, Bongers F, Burnham R, Putz FE, eds. *Ecology of Lianas*. Oxford: Wiley-Blackwell Publishers. pp. 253-287. DOI: https://doi.org/10.1002/9781118392409; e-ISBN:9781118392409

Angyalossy V, Pace MR, Evert RF, Marcati CR, Oskolski AA, Terrazas T, Kotina E, Lens F, Mazzoni-Viveiros SC, Angeles G, Machado SR, Crivellaro A, Rao KS,

Junikka L, Nikolaeva N, Baas P. 2016. IAWA List of Microscopic Bark Features. *IAWA Journal* **37**: 517-615. DOI: https://doi.org/10.1163/22941932-20160151

Barbosa ACF, Pace MR, Witovsk L, Angyalossy V. 2010. A new method to obtain good anatomical slides of heterogeneous plant parts. *IAWA Journal* **31**: 373-383. DOI: https://doi.org/10.1163/22941932-90000030

Barbosa ACF, Costa GRO, Angyalossy V, Dos Santos TC, Pace MR. 2018. A simple and inexpensive method for sharpening permanent steel knives with sandpaper. *IAWA Journal* **39**: 497-503. DOI: https://doi.org/10.1163/22941932-20170212

Bentham G, Hooker JD. 1876. *Genera plantarum* **2**: London: Reeve & Co. 1026-1053.

Bukatsch F. 1972. Bemerkungen zur Doppelfarbung Astrablau-Safranin. *Mikrokosmos* **61**: 255.

Callmander MW, Phillipson PB, Plunkett GM, Edwards MB, Buerki S. 2016. Generic delimitations, biogeography, and evolution in the tribe Coleeae (Bignoniaceae), endemic to Madagascar and the smaller islands od the western Indian Ocean. *Molecular Phylogenetics and Evolution* **96**: 178-186. DOI: https://doi.org/10.1016/j.ympev.2015.11.016

Carlquist S. 1982. The use of ethylenediamine in softening hard plant structures for paraffin sectioning. *Stain Technology* **57**: 311-317. DOI: https://doi.org/10.3109/10520298209066729

Carlquist S. 1985. Observations on functional wood histology of vines and lianas: Vessel dimorphism, tracheids, vasicentric tracheids, narrow vessels, and parenchyma. *Aliso* **11**: 139-157.

Carlquist S. 2001. *Comparative wood anatomy*. ed. 2, Berlin: Springer Verlag. DOI: https://doi.org/10.1007/978-3-662-04578-7; eISBN 978-3-662-04578-7

Carvalho-Francisco JN, Lohmann LG. 2020. Phylogeny and biogeography of the Amazonian *Pachyptera* (Bignonieae, Bignoniaceae). *Systematic Botany* **45**: 361-374. DOI: https://doi.org/10.1600/036364420X15862837791230

Chery JG, Pace MR, Acevedo-Rodríguez P, Specht CD, Rothfels CJ. 2020. Modifications during early plant development promote the evolution of nature's most complex woods. *Current Biology* **30**: 237-244. DOI: https://doi.org/10.1016/j.cub.2019.11.003

Crüger H. 1850. Einige Beiträge zur Kenntniss von sogenannten anomalen Holzbildungen des Dikotylenstammes. Erster Theil. *Botanische Zeitung* **8**: 98-168.

Darriba D, Taboada GL, Doallo R, Posada D. 2012. jModelTest 2: more models, new heuristics and parallel computing. *Nature Methods* **9**: 772. DOI: https://doi.org/10.1038/nmeth.2109

De Candolle AP. 1838. Revue sommaire de la famille des Bignoniacées. Tirée de la Bibliothèque Universelle de Genève. 1-24.

De Candolle AP. 1845. *Prodromus systematic naturalis regni vegetabilis* **9**: 142-248. Paris.

Dos Santos GMA, Miller RB. 1992. Wood anatomy of Tecomeae. *In:* Gentry AH, ed. *Bignoniaceae, Part II (Tribe Tecomeae)*. New York: New York Botanical Garden Press, Flora Neotropica Monograph 25. pp: 336-358

Dos Santos GMA, Miller RB. 1997. Wood anatomy of *Jacaranda* (Bignoniaceae): systematic relationships in sections monolobos and dilobos as suggested by twig and stem wood rays. *IAWA Journal* **18**: 369-383. https://doi.org/10.1163/22941932-90001502

Evert RF. 2006. Esau's plant anatomy: meristems, cells, and tissues of the plant body-their structure, function, and developmental. New Jersey: John Wiley and Sons. ISBN: 9780471738435

Fischer E, Theisen I, Lohmann LG. 2004. Bignoniaceae. *In*: Kubitzki K, Kadereit JK, eds. *The families and genera of vascular plants*. *VII. Dicotyledons. Lamiales (except Acanthaceae including Avicenniaceae)*. Heidelberg: Springer-Verlag. pp. 9-38 ISBN 978-3-642-18617-2

Fonseca LHM, Lohmann LG. 2015. Biogeography and evolution of *Dolichandra* (Bignonieae, Bignoniaceae). *Botanical Journal of the Linnean Society* **179**: 403-420. DOI: https://doi.org/10.1111/boj.12338

Fonseca LHM, Lohmann LG. 2018. Combining high-throughput sequencing and targeted loci data to infer the phylogeny of the "*Adenocalymma-Neojobertia*" clade. *Molecular Phylogenetics and Evolution* **123**: 1-15. DOI: https://doi.org/10.1016/j.ympev.2018.01.023

Gentry AH. 1980. Bignoniaceae - Part I (Crescentieae and Tourrettieae). *Flora Neotropica Monograph* **25**: 1-130.

Gentry AH. 1992. Bignoniaceae - Part II (Tribe Tecomae). *Flora Neotropica Monograph* **25**: 1-370.

Gerolamo CS, Angyalossy V. 2017. Wood anatomy and conductivity in lianas, shrubs and trees of Bignoniaceae. *IAWA Journal* **38**: 412-432. DOI: https://doi.org/10.1163/22941932-20170177

Grose SO, Olmstead RG. 2007a. Evolution of a charismatic Neotropical clade: molecular phylogeny of *Tabebuia* s.l., Crescentieae, and allied genera (Bignoniaceae). *Systematic Botany* **32**: 650-659. DOI: https://doi.org/10.1600/036364407782250553

Grose SO, Olmstead RG. 2007b. Taxonomic revisions in the polyphyletic genus *Tabebuia* s.l. (Bignoniaceae). *Systematic Botany* **32**: 660-670. DOI: https://doi.org/10.1600/036364407782250652

Hipkins VD, Tsai CH, Strauss SH. 1990. Sequence of the gene for the large subunit of ribulose 1,5-biphosphate carboxylase from the gymnosperm, Douglas fir. *Plant Molecular Biology* **15**: 505–507. DOI: https://doi.org/10.1007/BF00019168

IAWA Committee 1989. IAWA list of microscopic features for hardwood identification. *IAWA Bulletin* **10**: 219-332. DOI: https://doi.org/10.1163/22941932-90000496

Kaehler M, Michelangeli FA, Lohmann LG. 2012. Phylogeny of *Lundia* based on molecular and morphological characters. *Taxon* **61**: 368-380. DOI: https://doi.org/10.1002/tax.612008

Kaehler M, Michelangeli FA, Lohmann LG. 2019. Fine tuning the circumscription of *Fridericia* (Bignonieae, Bignoniaceae). *Taxon* **68**: 751-770. DOI: https://doi.org/10.1002/tax.12121

Kluge AG. 1989. A concern for evidence, and a phylogenetic hypothesis of relationships among Epicrates (Boidae, Serpentes). *Systematic Zoology* **38**: 7-25. DOI: https://doi.org/10.1093/sysbio/38.1.7

Kraus JE, Arduin M. 1997. *Manual básico de métodos em morfologia vegetal*. Seropédica, Rio de Janeiro: Editora Universidade Rural.

Li J. 2008. Phylogeny of *Catalpa* (Bignoniaceae) inferred from sequences of chloroplast *ndh*F and nuclear ribosomal DNA. *Journal of Systematics and Evolution* **46**: 341-348. DOI: https://doi.org/10.3724/SP.J.1002.2008.08025

Lohmann L. 2006. Untangling the phylogeny of neotropical lianas (Bignonieae, Bignoniaceae). *American Journal of Botany* **93**: 304-318. DOI: https://doi.org/10.3732/ajb.93.2.304

Lohmann LG, Taylor CM. 2014. A new generic classification of tribe Bignonieae (Bignoniaceae). *Annals of the Missouri Botanical Garden* **99**: 348-489. DOI: https://doi.org/10.3417/2003187

Maddison WP, Maddison DR. 2011. Mesquite: a modular system for evolutionary analysis. Version 2.75. https://www.mesquiteproject.org/

Meckes M, Garduño-Ramírez ML, Marquina S, Álvarez L. 2001. Iridoides adicionales de la planta medicinal *Astianthus viminalis* y su actividad hipoglucemiante y antihiperglucemiante. *Revista de la Sociedad Química de México* **45**: 195-199.

Medeiros MC, Lohmann LG. 2015. Phylogeny and biogeography of *Tynanthus* Miers (Bignonieae, Bignoniaceae). *Molecular Phylogenetics and Evolution* **85**: 3s2-40. DOI: https://doi.org/10.1016/j.ympev.2015.01.010

Miller MA, Pfeiffer W, Schwartz T. 2010. Creating the CIPRES Science Gateway for inference of large phylogenetic trees. *Gateway Computing Environment Workshop*: 1-8. DOI: https://doi.org/10.1109/GCE.2010.5676129

Olmstead RG, Sweere JA. 1994. Combining data in phylogenetic systematics: an empirical approach using three molecular data sets in the Solanaceae. *Systematic Biology* **43**: 467-481. DOI: https://doi.org/10.2307/2413546

Olmstead RG, Zjhra ML, Lohmann LG, Grose SO, Eckert AJ. 2009. A molecular phylogeny and classification of Bignoniaceae. *American Journal of Botany* **96**: 1731-1743. DOI: https://doi.org/10.3732/ajb.0900004

Olmstead RG. 2013. Phylogeny and biogeography in Solanaceae, Verbenaceae and Bignoniaceae: a comparison of continental and intercontinental diversification patterns. *Botanical Journal of the Linnean Society* **171**: 80-102. DOI: https://doi.org/10.1111/j.1095-8339.2012.01306.x

Pace MR. 2019. Optimal preparation of tissue sections for light-microscopic analysis of phloem anatomy. *In:* Liesche J, ed., *Phloem: Methods in Molecular Biology*. New York: Humana.Pp. 3-16 DOI: https://doi.org/10.1007/978-1-4939-9562-2_1; e-ISBN 978-1-4939-9562-2

Pace MR, Angyalossy V. 2013. Wood anatomy and evolution: a case study in the Bignoniaceae. *International Journal of Plant Sciences* 147: 1014-1048. DOI: https://doi.org/10.1086/670258

Pace MR, Lohmann LG, Angyalossy V. 2009. The rise and evolution of the cambial variant in Bignonieae (Bignoniaceae). *Evolution & Development* **11**: 465-479. DOI: https://doi.org/10.1111/j.1525-142X.2009.00355.x

Pace MR, Lohmann LG, Angyalossy V. 2011. Evolution of disparity between the regular and variant phloem in Bignonieae (Bignoniaceae). *American Journal of Botany* **98**: 602-618. DOI: https://doi.org/10.3732/ajb.1000269

Pace MR, Lohmann LG, Olmstead RG, Angyalossy V. 2015a. Wood anatomy of major Bignoniaceae clades. *Plant Systematics and Evolution* **301**: 967-995. DOI: https://doi.org/10.1007/s00606-014-1129-2

Pace MR, Lohmann LG, Alcantara S, Angyalossy V. 2015b. Secondary phloem diversity and evolution in Bignonieae (Bignoniaceae). *Annals of Botany* **116**: 333-358. DOI: https://doi.org/10.1093/aob/mcv106

Pace MR, Zuntini AR, Lohmann LG, Angyalossy V. 2016.

Phylogenetic relationships of enigmatic *Sphingiphila* (Bignoniaceae) based on molecular and wood anatomical data. *Taxon* **65**: 1050-1063. DOI: https://doi.org/10.12705/655.7

Pérez-Gutiérrez RM, Vargas Solis R, Garcia Baez E & Gallardo Navarro Y. 2009. Hypoglycemic activity of constituents from *Astianthus viminalis* and streptozotocin-induced diabetic mice. *Journal of Natural Medicines* **63**: 393-401. DOI: https://doi.org/10.1007/s11418-009-0343-7

R Core Team. 2020. R: A language and environment for statistical computing. R Foundation for Statistical Computing, Vienna, Austria. URL: https://www.R-project.org/

Ragsac AC, Farias-Singer R, Freitas LB, Lohmann LG, Olmstead RG. 2019. Phylogeny of the neotropical tribe Jacarandeae (Bignoniaceae). *American Journal of Botany* **106**: 1-13. DOI: https://doi.org/10.1002/ajb2.1399

Rasband WS. 2012. ImageJ. Program distributed by the author. U. S. National Institutes of Health. http://imagej.nih.gov/ij

Rambaut A. 2010. FigTree v1.3.1. Institute of Evolutionary Biology, University of Edinburgh, Edinburgh. Available at: http://tree.bio.ed.ac.uk/software/figtree/ (Accessed August 25, 2018).

Rambaut A, Drummond AJ, Xie D, Baele G, Suchard MA. 2018. Posterior summarization in Bayesian phylogenetics using Tracer 1.7. *Systematic Biology* **67**: 901–904. DOI: https://doi.org/10.1093/sysbio/syy032

Record SJ, Hess RW. 1943. Timbers of the new world. New Haven: Yale University Press. ISBN 0405028067

Ronquist F, Teslenko M, Van Der Mark P, Ayres DL, Darling A, Höhna S, Larget B, Liu L, Suchard MA, Huelsenbeck JP. 2012. MrBayes 3.2: Efficient bayesian phylogenetic inference and model choice across a large model space. *Systematic Biology* **61**: 539-542. DOI: https://doi.org/10.1093/sysbio/sys029

Roth I. 1981. Structural patterns of tropical barks. *In:* Braun HJ, Carlquist S, Ozenda P, Roth I, eds. *Encyclopedia of Plant Anatomy*. Berlin: Gebrüder Bornstraeger. ISBN 3443140122

Rupp P. 1964. Polyglykol als Einbettungsmedium zum Schneiden botanischer Präparate. *Mikrokosmos* **53**: 123-128.

Schenck H. 1893. Beiträge zur Biologie und Anatomie der Lianen im Besonderen der in Brasilien einheimischen Arten. II. Theil. Beiträge zur Anatomie der Lianen. *In*: Schimper AFW, ed. *Botanische Mittheilungen aus den Tropen*. Jena: Gustav Fisher.

Spangler RE, Olmstead RG. 1999. Phylogenetic analysis of Bignoniaceae based on the cpDNA gene sequences *rbc*L and *ndh*F. *Annals of the Missouri Botanical Garden* **86**: 33-46. DOI: https://doi.org/10.2307/2666216

Stamatakis A. 2014. RAxML version 8: A tool for phylogenetic analysis and post-analysis of large phylogenies. *Bioinformatics* **30**: 1312-1313. DOI: https://doi.org/10.1093/bioinformatics/btu033

Taberlet P, Gielly L, Pautou G, Bouvet J. 1991. Universal primers for amplification of three non-coding regions of chloroplast DNA. *Plant Molecular Biology* **17**: 1105-1109. DOI: https://doi.org/10.1007/BF00037152

Thiers B. 2017 [continuously updated]. Index herbariorum: a global directory of public herbaria and associated staff. New York Botanical Garden's Virtual Herbarium. http://sweetgum.nybg.org/science/ih/ (accessed 29 November 2020).

Thode VA, Sanmartín I, Lohmann LG. 2019. Contrasting patterns of diversification between Amazonian and Atlantic forest clades of Neotropical lianas (*Amphilophium*, Bignonieae) inferred from plastid genomic data. *Molecular Phylogenetics and Evolution* **133**: 92-106. DOI: https://doi.org/10.1016/j.ympev.2018.12.021

Zjhra ML, Sytsma KJ, Olmstead RG. 2004. Delimitation of Malagasy tribe Coleeae and implications for fruit evolution in Bignoniaceae inferred from a chloroplast DNA phylogeny. *Plant Systematics and Evolution* **245**: 55-67. DOI: https://doi.org/10.1007/s00606-003-0025-y

Associate editor: Silvia Aguilar Rodríguez

Author contributions: MRP, conceptualization, methodology, field work, morpho-anatomical analysis, writing of original draft, funding acquisition; BHH, molecular methods and analysis, validation, data curation; EMMS, field work, validation; LGL, methodology validation, DNA alignments of Bignoniaceae, writing, review and editing; NIC; conceptualization, methodology, molecular methods and analysis, validation, data curation, writing, review and editing, funding acquisition.